SYMPOSIUM ON SIMULATION IN ARCHITECTURE + URBAN DESIGN
SimAUD 2020

# Climate Change Impact on Multi-Objective Optimization: A Case Study on Educational Buildings

**Şahin Akın[1,a], Orçun Koral İşeri[1,b], Çağla Meral Akgül[2], Bilge Erdoğan[3], İpek Gürsel Dino[4]**

[1] Ph.D. Students, First Co-Authors
METU, Ankara, Turkey
akin.sahin[a], koral.iseri[b] @metu.edu.tr

[2] Assist. Prof. Dr.,
METU, Ankara, Turkey
cmeral@metu.edu.tr

[3]Assoc. Prof. Dr.,
HWU, Edinburgh, UK
b.erdogan@hw.ac.uk

[4]Assoc. Prof. Dr.,
METU, Ankara, Turkey
ipekg@metu.edu.tr

**ABSTRACT**
The changing weather conditions due to global climate change is expected to have a direct impact on buildings' energy demand and occupant comfort. These conditions are estimated to become more challenging for educational facilities due to their high occupant density and the students' sensitivity to heat. This study aims to present an approach for a comparative analysis for multi-objective optimization results that are projected under different climate change conditions. Two separate optimization processes were performed using NSGA-II for an existing educational building, with the goal of minimizing occupant discomfort and energy use. The differences between the resulting Pareto-sets were analyzed based on the hypervolume difference and statistical evaluations, including the T-test and the distribution of properties. The results of the two optimization processes showed that future weather conditions should be considered on the retrofit process as two Pareto-set have resulted differently in terms of decision variable values and the hypervolume calculation. The discomfort hours ($Y_{1\text{-Current}}$) for optimization with current data resulted in lower values compared to the optimization with projected data ($Y_{1\text{-Projected}}$), on the contrary, the total energy demand ($Y_{2\text{-Current}}$) objective results have resulted in higher values than the projected data results ($Y_{1\text{-Projected}}$).

**Author Keywords**
Climate Change; Multi-Objective Optimization; Occupant Comfort; Building Retrofits

**ACM Classification Keywords**
I.6.4 [Simulation and Modeling]: Model Validation and Analysis; I.6.5 [Simulation and Modeling]: Model Development – Modeling methodologies

## 1 INTRODUCTION

The greenhouse gas emission level has reached its highest level since the industrial revolution, and it continues to rise [10]. The increasing emissions have a negative influence on Earth's climate system, and this situation threatens the livability in the built environment. Concerning this situation, many buildings are required to be adapted [13,14], and the building sector needs performance-based planning and renewal to cope with the changing climate conditions. Particularly, buildings' energy performance parameters (e.g., the efficiency of the lighting fixtures, infiltration, and surface heat transfer rates) should be reconsidered for better-performing buildings in the future. Building retrofits plays a critical role in upgrading existing buildings' performances. It should be conducted in a well-planned way to maximize performance and minimize environmental impact. In the literature, it is reported that there is a trade-off between performance parameters, and reaching optimal solutions based on contradicted performance objectives is challenging [7]. However, optimization algorithms could provide an advantage to facilitate achieving optimal solutions. Therefore, optimization is an important technique for the identification of the performance parameter values that can satisfy performance objectives [10].

Energy performance and occupant comfort of buildings may change over the years as a consequence of global climate change. Therefore, the planned retrofit activities should also be responsive to climate change. Notably, it is vital to observe these changes in educational buildings since these buildings host many different users. Even though studies on energy efficiency and reduction of environmental impact in the built environment are increasing, only a few studies are conducted for educational facilities to evaluate and observe energy demand and occupant comfort levels [18].

Comparative studies play a significant role in retrofit planning of the buildings [11,17]. Due to global climate change, the outside temperature conditions are changing, and it has critical effects on the indoor comfort, energy demand, and environmental impact of buildings [8]. Therefore, changing weather conditions should also be considered during retrofit processes by comparing the retrofit scenarios' current and future performances. In this work, the authors realize this comparison with a multi-objective optimization process for an educational facility.

The study aims to realize a multi-objective optimization methodology with the objectives of the calculation of discomfort hours ($Y_1$) in the ASHRAE 55-2004's summer or winter clothes region [3] and the total energy demand ($Y_2$) for two climate conditions, e.g., current and projected future weather. The two Pareto-set of the optimizations were analyzed based on Pareto-set hypervolume calculation and the statistical data distribution differences. The presented

SimAUD 2020 May 25-27, Online

approach may help decision-makers making sense of optimization results under different climatic conditions.

## 2 LITERATURE REVIEW

The building retrofit studies focus on thermal comfort, visual comfort, acoustic performance, and indoor air quality, depending on passive and active interventions to architecture [1,6]. Educational facilities are complex buildings that contain various space types such as classrooms, studios, offices, common areas, requiring different demands. Retrofit processes' performance objectives require alternative interventions for responding to the varying demands of these spaces. Retrofit actions' impact on environmental performance, the relationships between performance objectives, and performance parameters can be realized through optimization studies effectively [10,12].

### 2.1 Climate Impact on Buildings

Weather information is essential in building energy simulations, as it has a significant influence on energy usage and occupant comfort. As global climate change is expected to have a drastic impact on the environmental conditions in the long term, the energy performance of the buildings is expected to change accordingly. Recent studies have aimed to analyze the effects of climate change for buildings under future climate conditions, to propose improvements at building systems [16,20]. Besides, the potential changes in weather conditions may have some economic consequences that stakeholders of buildings required to deal with [19].

### 2.2 Optimization and Building Energy Efficiency

Buildings consist of multiple systems and components; therefore, many different retrofit scenarios can be proposed to improve user comfort, reduce energy demand, and environmental impact [10]. Optimization algorithms are widely used in the literature, as they can change multiple variables in a single model at the same time and compute the solution set based on multiple objectives [9,15]. Consequently, designers may select the optimal results according to their priorities from the solution clusters, namely Pareto-set, during the design process [10]. However, decision-making based on different Pareto-sets is a hitherto unaddressed problem. Besides, changing weather conditions may also adversely affect the selection of optimum parameters. Therefore, this study aims to present an approach to interpret the differences between current and future climate conditions in the optimization processes.

## 3 METHODOLOGY

This section explains the methodological framework for the comparison of two optimization processes for building energy simulations with different climate conditions based on the hyper-volume technique and statistical analysis of the Pareto-set distributions. In this regard, a case study building was selected, through which the approach was presented.

### 3.1 Description of the Case Study

The case study was selected as the Faculty of Architecture building at the Middle East Technical University, Ankara. Anakara is in Ashrae climate zone 4B (CDD10ºC ≤ 2500 AND HDD18ºC ≤ 3000) [2] and has a dry continental climate with hot summers and cold, snowy winters. Exposed concrete curtain walls, large glass surfaces, brise soleil façades, flat roof, and open plan are the architectural features of this building. The building contains several departments, including architecture, industrial design, and city planning (Figure 1). These spaces are heated from late fall to late spring using a central heating system. The heating system is central to the whole campus, and it runs on natural gas. Fan coil units are used for larger spaces, and radiators were used for smaller spaces to heat the building. Besides, the building does not have any active cooling or mechanical ventilation systems, and the simulations were performed, excluding mechanical ventilation and air conditioning's energy demands.

### 3.2 Energy model setup

For the building energy simulations and optimization, DesignBuilder [21] was used. For optimizations, the building was only partially modeled in building energy software. The total simulated area was 3733 m$^2$, including four different zone types such as classrooms, design studios, meeting rooms, and circulation areas, which are occupied dependent on the course hours. However, some places, especially the studios, are extensively occupied even after the course hours.

The building contains numerous volumes and thermal zones, which can result in elongated simulation periods that can challenge the multi-objective optimization process. Therefore it was necessary to first simplify the energy model by combining zones with similar characteristics into a single zone. For instance, classes next to each other were lumped to a single zone. Another simplification act was performed on the shading elements on the west-facing zones. The perforated geometry of these elements was found to increase the simulation time significantly. Therefore, the shading elements were replaced with planar surfaces with reduced opacity. These planar elements ensured that the simulation complexity is reduced while emulating the shading behavior of the actual shading elements. Several energy simulations were conducted to determine the opacity level required for building geometry. The opacity parameter of the surface was decreased gradually until achieving a realistic alternative (Table 1).

| Shading | Solar gain (kWh/m2) |
|---|---|
| Baseline Detailed | 197.02 |
| Combined Class, % 60.4 opaque | 197.16 |

**Table 1.** Analysis for simplified shading geometry for the optimization model

The simulation analysis period was set to six months. As seen in Figure 3, February has the coldest temperature values, and there is symmetrical temperature distribution before and after August. Therefore, the simulation period was set to February 1 – August 1.

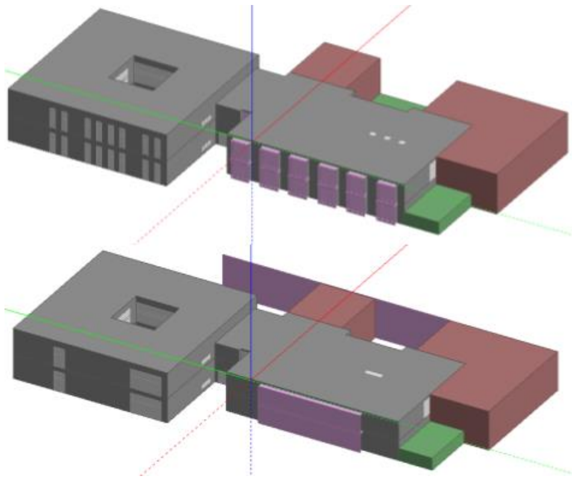

**Figure 1.** Detailed energy model of METU's architecture faculty (top); Simplified model of the faculty (bottom)

### 3.3 Optimization and The Selection of Parameters

In terms of energy efficiency and occupant comfort, the variables were determined separately as a single scenario; then, all scenarios are combined under an optimization model. The combination of scenarios in the optimizations was found useful to increase the retrofit actions' impact and to understand how the different scenarios work together. Table 2 shows the selected decision variables and optimization objectives.

As seen in Table 2, the decision variables can take continuous or discrete values, and as-is building's conditions are changed in the simulations by different decision variables. The seven decision variables' values were assigned as discrete values: $X_2$ (0.00001, 0.0006, 0.000140, 0.000160 kg/s.m@1Pa), $X_4$ (with combined parameter values, including U-values ranging from 0.6 to 2.6; SHGC values ranging from 0.5 to 0.8), $X_5$ (with different types, including low to high transmittance; low to high reflectance values for the shading material), $X_6$ (with different types, including overhangs ranging in length 0.5 to 1 m or sidefins ranging from 0.5 to 1 m; louvres ranging from 0.25 to 0.5 m), $X_7$ (with combined parameter values, including insulation thicknesses ranging from 4 cm to 16 cm; outmost coating with reflective or non-reflective paint), $X_8$ (with combined parameter values, including insulation thicknesses ranging from 0 to 16 cm; outmost coating with reflective or non-reflective paint), $X_9$ (with combined parameter values, including aluminum, wooden, PVC materials; frame thicknesses ranging from 5 to 60 mm).

The solutions are evaluated by two objective functions, namely the minimization of the total energy demand (kWh) and minimization of the discomfort hours. It is important to state that there is also a trade-off between these two objectives. The discomfort hours ($Y_1$) is calculated by summing up the exceeded degree differences from 28°C, which is determined as the top limit for the comfortable indoor temperature for all seasons [3]. The objective of total energy demand ($Y_2$) contains heating and lighting demands only since the building does not have active mechanical ventilation and cooling system. Also, the defined retrofit scenarios do not focus on changing electricity consumption; therefore, the $Y_2$'s results can only be evaluated over changes in heating energy consumption.

| | Selected Retrofit Scenarios | As-is building | Range |
|---|---|---|---|
| $X_1$ | Opening Ratio of Interior Windows to increase cross Ventilation | 0% | 0% - 90 % |
| $X_2$ | Air Tightness (infiltration) | 0.001 kg/s.m @1Pa | 4, Discrete |
| $X_3$ | Opening Ratio of Exterior Windows to increase natural ventilation | 15% | 10% - 90 % |
| $X_4$ | Glazing Types (with different SGHC, U-value) | 2.6 U-value, | 36, Discrete |
| $X_5$ | Shading Types, Interior (with different transmittance and reflectance values) | Non-reflect. Drapes | 6, Discrete |
| $X_6$ | Shading Types, Exterior (with different depth and shading type) | Brise-soleils | 6, Discrete |
| $X_7$ | Roof Insulation (with reflective coating layer) | 4cm non reflective insulation | 8, Discrete |
| $X_8$ | Wall Insulation (with reflective coating layer) | 3.316 U-value | 8, Discrete |
| $X_9$ | Window Frame Types (with different thickness and material type) | 40 mm Aluminum | 9, Discrete |
| **Selected Objective Functions** | | | |
| $Y_1$ | Discomfort Hours (hours) according to ASHRAE [3] | | |
| $Y_2$ | Total energy demand (kWh) | | |

**Table 2.** Decision variables and objectives

### 3.4 Optimization Algorithm and Energy Simulations

In this study, DesignBuilder's optimization module that implements the Non-Dominated Sorting Genetic Algorithm-II (NSGA-II) was used. NSGA-II is a multi-objective genetic algorithm that can maintain a spread of solutions and converge in the obtained nondominated front [7]. In this study, the algorithm aims to minimize the total energy demand ($Y_1$) and minimize the discomfort hours ($Y_2$) simultaneously.

Figure 2 presents the flowchart of the NSGA-II genetic algorithm's working process. In the first step, the population ($R_t$) is generated with $P_t$ and $Q_t$. The population is sorted based on the non-domination rule with elitism. The $F_1$ set is formed by best-nondominated solutions. The members of the new population $P_{t+1}$ are selected from $F_1$, and if needed, from $F_2$ and $F_3$. Then, the new population $P_{t+1}$ with the size $N$ is used for selection, crossover, and mutation to form a new population $Q_{t+1}$ of size $N$ as the next generation. The selection criteria of members works according to the crowded-comparison rule in which calculating the rank and crowded-distance of each solution as generating $P_{t+1}$.

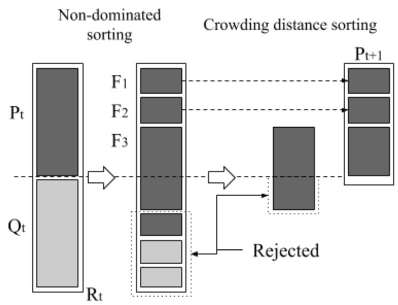


**Figure 2.** NSGA-II optimization loop [7]

### 3.5 Weather Data

The account for the impact of climate change on building performance, the future weather data was generated using Weathershift [5]. Weathershift transforms existing weather datasets (.epw files) based on different greenhouse gas emission projections in a procedure named 'morphing'. The process alters current weather variables to produce future weather time series. Morphing preserves the actual weather sequences of the current weather data. Offset data is a climate projection generated by Coupled Model Intercomparison Project Phase 5 (CMIP5). These models are defined as Representative Concentration Pathways (RCP). For instance, RCP 8.5 is the business-as-usual scenario as a worst-case scenario. In this study, the RCP 8.5 scenario was used to observe the climate impact on the retrofit process.

The current and projected weather data were used to compare climate change impact on educational facilities in terms of retrofit scenario evaluation using evolutionary algorithms. The two weather files represent two different periods. The first one represents the current weather conditions. The second represents the future weather conditions that are projected for the year 2060. The current and projected outside dry bulb temperature values can be seen in Figure 3.

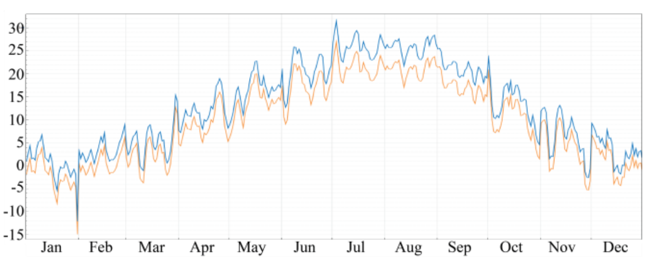


**Figure 3.** Dry-bulb temperature (C°); Current weather data (Orange), Projected weather data (Blue)

### 3.6 The Hypervolume Difference Indicator

The hypervolume indicator is used in this paper to compare the two Pareto-front sets of the two optimization results. The method calculates the volume of the dominated region of the distribution of the objective functions [4]. The comparison of two optimization results is the difference between the hypervolume area based on the total energy demand and the total number of discomfort hours (1). This sort of comparison method was used to compare different optimization sets between each other only since it is unitless.

$$\Delta I = |I_i - I_f| \quad (1)\ [4]$$

where $\Delta I$ is the region difference between two multi-objective optimization areas based on the previous formula. $I_i$ is the area of optimization with current weather data, and $I_f$ is the optimization with projected weather data.

### 3.7 The statistical Evaluation of the Pareto-sets

As an alternative comparison method, the distribution of the two Pareto-set is analyzed based on statistical tests, i.e., kurtosis, skewness value comparison. The results also were presented on the box plot. The dominated solutions were not included in the observation. In addition to the skewness and kurtosis analysis, the Paired Sample T-test were used. T-Test presents univariate comparative descriptive statistics (mean, std. deviation) for each variable of the test [14]. The test is a statistical method for understanding whether the mean difference between the two situations is significant.

## 4 RESULTS AND DISCUSSION

This section presents the results of two optimization processes and their differences in terms of hypervolume and statistical analysis. The execution time was approximately four days for each optimization process. The population and initial random population sizes were determined as 100 individuals. After the 70th generation, no improvement was observed. It is important to note that a brute-force calculation would take approximately 9538 days for the same parameter set. As a result, a significant reduction in the computation time was achieved by applying the optimization algorithm. For comparison of the optimization results, the highest values on the Pareto-set in terms of objective functions were presented. In Figure 4, the highest value according to $Y_1$ was circled and shown as 1. Besides, the highest value according to $Y_2$ and shown as 2. Subsequently, statistical analyses were applied to compare the distribution of Pareto-set results. Finally, the area differentiation between two Pareto-sets was calculated by the hypervolume difference.

### 4.1 Optimization with the Current Weather Conditions

The optimization process of the current weather condition has produced 49 optimum results. As a result of the optimization with the current dataset, while the discomfort hours ($Y_{1\text{-Current}}$) were found between 1005 and 2321 hours, the total energy demand ($Y_{2\text{-Current}}$) demand values were between 37.06 kWh/m$^2$, and 47.16 kWh/m$^2$ (Figure 4). The discomfort hours resulted in more than 1000 hours. These results could be explained by the fact that the selected building was built in the *1960s*, and does not have any wall or floor insulation. Moreover, the lack of air conditioning and inefficient natural ventilation also contributed to high overheating.

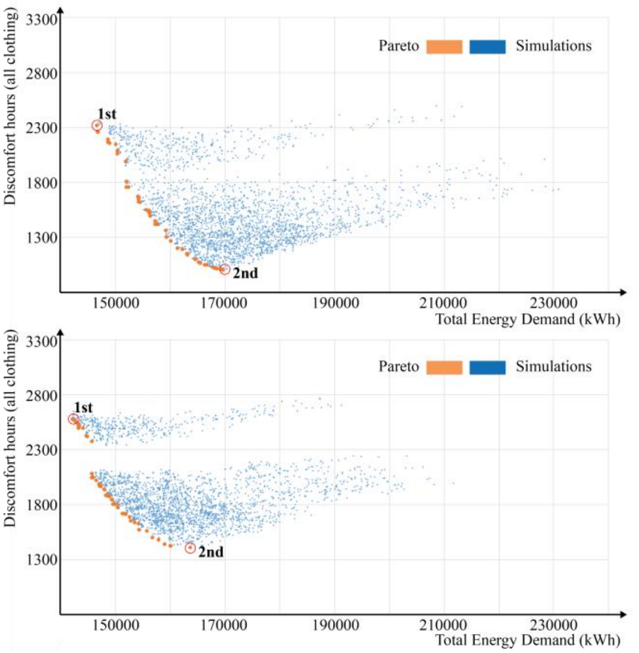


**Figure 4.** Current Weather Data optimization results (top); Projected weather data optimization results (bottom)

According to the simulation results, $Y_{1\text{-Current}}$ was calculated as 2261 hours, and $Y_{2\text{-Current}}$ was calculated as 37.08 kWh/m$^2$ for the highest value, according to $Y_1$. These results from the Pareto-set tend to increase envelope thermal resistance in terms of selecting the highest-performance of infiltration ($X_2$) and decreasing external window opening ratios ($X_3$) to 0%. Also, the algorithm chose decision variable alternatives for benefiting from solar gains, such as increasing the SGHC value for the glazing types ($X_4$), and using shorter exterior overhang shading alternatives ($X_6$). On the other hand, $Y_{1\text{-Current}}$ emerged as 1010 hours, and $Y_{2\text{-Current}}$ emerged as 42.78 kWh/m$^2$, as it is the highest value, according to $Y_2$. This optimum result consists of the envelope with less thermal resistance, medium level natural ventilation, and infiltration decision variable selection, e.g., low-performance infiltration selection ($X_2$) and increasing external window opening ratios ($X_3$) to 90%. On the contrary, the level of solar gain benefit could be reduced by choosing the longer overhang shading alternative ($X_4$) and by decreasing the SGHC value for the glazing type ($X_4$).

Finally, similar decision variable values were observed for the two Pareto-set comparisons. For instance, the internal window opening ratio ($X_1$) resulted in a 90% openness ratio, and the window frame thickness ($X_4$) was 60 mm for all Pareto results. Besides, non-reflective outmost materials for the flat roof construction ($X_7$) resulted in both optimizations.

### 4.2 Optimization with Future Weather Conditions

During the optimization process with the future weather file, 49 different Pareto solutions were generated. The 2$^{nd}$ optimization Pareto-set resulted between 1407 hours and 2576 hours for $Y_{1\text{-Projected}}$; $Y_{2\text{-Projected}}$ results varied between 35.92 to 45.50 kWh/m$^2$ (Figure 4). By observing the Pareto-front results, the decision variables, including the infiltration ($X_2$), opening ratio exterior window ($X_3$), shading types-exterior ($X_6$), window frame types ($X_9$) had multiple values instead of converging only on a single value. On the other hand, the decision variables, including the opening ratio of interior windows ($X_1$), windows' blind types ($X_5$), roof insulation ($X_7$), wall insulation ($X_8$) were positioned in a narrow scale by having similar values, e.g., "90% opening ratio of the interior windows with high reflectance – low transmittance window blind types".

To explain the distribution of the results in more detail, the presentation of the two extreme points on the Pareto-set helps. The first extreme resulted in one of the highest points of the Pareto-set, where $Y_{1\text{-Projected}}$ was 2573 hours, and $Y_{2\text{-Projected}}$ was 39.57 kWh/m$^2$. This solution has the lowest infiltration rates among the other solutions ($X_2$), and the thickest window frame type option ($X_9$) in the decision variables. Similarly to the optimization with current weather data, there was a tendency to increase thermal resistance on the envelope. In parallel with this situation, alternatives were chosen to provide more benefit from solar gain in terms of decision variables, i.e., reducing the SHGC value ($X_4$) and using shorter overhang shading depth ($X_6$). Lastly, the non-reflective wall insulation options were found effective to receive heat gains from vertical surfaces.

The second extreme had one of the lowest values in the Pareto-front trend line and had $Y_{1\text{- Projected}}$ of 1559 hours, and $Y_{2\text{- Projected}}$ of 43.30 kWh/m$^2$. On the contrary, this result consists of the highest infiltration rates among the other solutions ($X_2$), and has a thinner window frame thicknesses as 50 mm compared to the first extreme's $X_9$ decision variable. Some of the results were close to the $Y_1$ by generating less heat resistance on the envelope. On the other hand, some of the results concluded as more focused on $Y_2$ by using thicker insulations.

### 4.3 Comparison of Pareto-set solutions

According to Figure 4, it can be seen that the Pareto-sets were horizontally separated into two parts because of the differences in decision variables' effects on the simulations' performances. For the optimization with current weather data, the upper part of the Pareto-set resulted in between 1956 to 2321 hours, and the lower part of the Pareto-set resulted in between 1005 to 1807 hours in terms of the discomfort hours objective. For the optimization with projected data, the upper part resulted in between 2371 to 2575 hours, and the lower part resulted between 1407 to 2083 discomfort hours.

The projected weather data contains higher dry-bulb temperatures and irradiation values as compared to current weather data. Therefore, the total energy demand values were resulted in lower compared to the projected weather data optimization since the building demands lower heating energy consumption. On the other hand, the discomfort hours were found higher in number because of the increased outside temperature values for the projected weather data.

According to Figure 5, the calculated region of all solutions for current weather data was found as 83247140, and it was found as 62607314 for the optimization with projected data (1). Therefore, the hypervolume difference between the two ($\Delta I$) was found as 20639826 (2). The current weather data's Pareto-front set positioned closer to the origin (0,0) compared to the optimization with projected-data. For two optimization processes, the Pareto-set distributions were performed similarly in terms of the ranges of objective functions, instead of the distribution values. Nevertheless, the distribution of the Pareto-set was different for two optimizations as the current data's results were lower for $Y_1$. On the contrary, for the projected weather data, $Y_2$ resulted in lower values. The optimization with the current weather data's solution cluster dominantly covered more areas than the projected weather data's solution cluster. This can be explained with the high outside temperatures in projected weather data, which affect the distribution of the solution cluster.

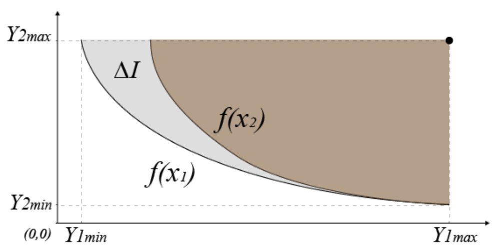


**Figure 5.** Hypervolume Indicator (H*v*) difference between two multi-objective optimization Pareto-front set

### 4.4 An analysis of the decision variables on the Pareto-fronts

In the Pareto-sets, the frequency rate of several variables was found higher than the rest. This finding indicates that the recurring variables in the Pareto-sets have the potential in terms of high performance for both optimizations. Accordingly, the opening ratio of the interior windows ($X_1$), window types ($X_4$), roof insulation ($X_7$), wall insulation ($X_8$) decision variables' values were observed similarly in both of the optimizations. Particularly for $X_7$ and $X_6$, compared to the non-insulated existing conditions of the building, the highly insulated alternatives in terms of high resistance to thermal transfer perform better for the current and projected weather of Ankara. Similarly, the window alternatives with low U-values were observed more in the Pareto-sets. Also, the opening ratio of the interior windows ($X_1$), which helps reduce interior discomfort hours, was selected with a %90 openness rate for both of the optimizations. On the other hand, for some decision variables, there was no definite dominant selection for both optimizations, i.e., window frame types ($X_2$) and interior shading types ($X_5$) and exterior shading types' ($X_6$).

Apart from this, when the $X_3$ decision variable was examined in both Pareto-sets, the number of discomfort hours increased as the openness rate approached 0%, and the number of discomfort hours decreased as it approached 90%. The Pareto-sets' results showed that some decision variables were more impactful in terms of changing the total energy and discomfort hours. Strikingly, the infiltration performance parameter was observed as the most dominant decision variable among the other scenarios, which drastically effects the overall building performance. Also, exterior shading types ($X_6$) more dominantly had a more impact on the objective values for both optimizations compared to the interior shading types ($X_5$).

On the other hand, window frame types' ($X_2$) material parameters were generally observed with PVC since the material has better heat transfer values compared to the other defined alternatives. However, the frame thickness parameter varied between 0,005 to 0,060 meters. This variation was observed more, especially in the Pareto-set with the current weather data.

### 4.5 Statistical Comparison of the Two Generated Data Sets

Multi-objective optimization aims to search for non-dominated results based on decision variables. Therefore, objective functions should be analyzed based on the difference between the two Pareto-sets. Figure 6 shows the Pareto-set results of the optimizations on the box plot with groups of data based on quartiles.

The optimization with current data's Pareto-set's $Y_{1\text{-Current}}$ took values between 1300 and 1650 hours, and the optimization with projected data's Pareto-set's $Y_{1\text{-Projected}}$ took values between 1800 and 2050 hours for the interquartile range. Both objectives of the optimizations, the outlier values were positioned closer to the upper-extreme values. The Pareto-set of current data values started from up to 2000 discomfort hours, and for the Pareto-set of the projected data values, they started from up to 2400 discomfort hours.

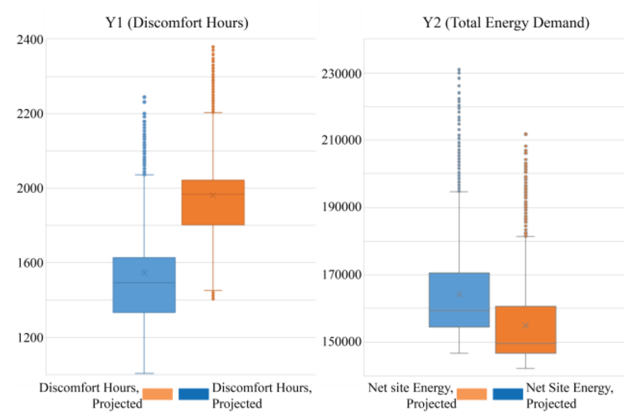


**Figure 6.** Objective functions distributions on box-plot; $Y_1$ based on ASHRAE 55 calculation (left), $Y_2$ (right) [20]

Further, $Y_{2\text{-Current}}$ results were distributed in a broader range between 43.10 kWh/m$^2$ to 47.27 kWh/m$^2$. However, $Y_{2\text{-Projected}}$ values took values between 40.87 kWh/m2 and 44.50 kWh/m2. The difference for two optimizations caused by a similar reason that was the higher values of weather conditions in terms of outside dry-bulb temperature (C°). For the outlier values, the 1st optimization objective values started from 52.84 kWh/m$^2$, and the 2nd optimization objective values started from 44.50 kWh/m$^2$, so its results ended up in a narrower area.

| | N | Mean | SD | Skewness | Kurtosis |
|---|---|---|---|---|---|
| $Y_{2\text{-Current}}$ | 49 | 39.78 | 1.70 | 0.225 | -1.011 |
| $Y_{2\text{-Projected}}$ | 49 | 35.93 | 1.29 | 0.837 | 0.300 |

**Table 3.** Distribution Properties of Objective Pareto Set ($Y_2$)

As seen in Table 3, the distribution properties of $Y_{2\text{-Current}}$ are positively less skewed; on the contrary, the results with $Y_{2\text{-Projected}}$ were found as highly positively skewed. Both optimization distributions were generally populated to the lower total energy demand values. For the kurtosis evaluation, $Y_{2\text{-Current}}$ had a negative value, which can be explained that the distribution had a high peak than the usual. However, $Y_{2\text{-Projected}}$ had a positive kurtosis value that was flatter than the usual, which means that they were equally distributed between the boundaries of the total energy demand results.

| | N | Mean | SD | Skewness | Kurtosis |
|---|---|---|---|---|---|
| $Y_{1\text{-Current}}$ | 49 | 1537 | 416 | 0.411 | -1.097 |
| $Y_{1\text{-Projected}}$ | 49 | 1929 | 342 | 0.534 | -0.581 |

**Table 4.** Distribution properties of objective Pareto-set ($Y_1$), ASHRAE 55 [20]

In Table 4, the normal distribution properties of the discomfort hours objective function ($Y_1$) were positively skewed for both of the results with $Y_{1\text{-Current}}$ and $Y_{1\text{-Projected}}$. Consequently, the optimization algorithm could reach lower values for $Y_1$. For kurtosis evaluation, each objective function in two optimizations valued as negative, which means the distribution has a high peak than the normal. It can be said that the objective values were evaluated close to average.

| $Y_{1\text{-Current}}$ & $Y_{1\text{-Projected}}$ | |
|---|---|
| Mean | -538 |
| SD (σ) | 94 |
| %95 C.I. Difference | -566 (Lower), -511 (Upper) |
| $t_{49}$ | -39.781 |
| d*f* | 48 |
| Sig. (2-tailed) | .000 |
| Correlation | 0.964 |

**Table 5.** Paired sample t-test of discomfort hours, ASHRAE 55 function Pareto-set

Table 5 presents the results of $Y_2$ for the two Pareto-sets ($r=0.964$, $p<0.001$). The distribution of two Pareto-set was strongly correlated similarly to the $Y_1$ comparison. There was a significant difference in the average values between two Pareto-front distributions ($t_{49} = -39.781$, $p < 0.001$). On average, the objective function of the current weather data optimization was 538 discomfort hours lower than the optimization with the projected weather data (95% CI [-566, -511]). The lower temperature values for the projected weather data directly affected the $Y_1$'s Pareto-set values.

In Table 6, the two optimization processes' total energy demand values were positively and strongly correlated to each other ($r=0.970$, $p<0.001$). Also, there was an important statistical difference in average values between two Pareto-front distributions ($t_{49} = 36.313$, $p < 0.001$).

| $Y_{2\text{-Current}}$ & $Y_{2\text{-Projected}}$ | |
|---|---|
| Mean | 1.47 |
| SD (σ) | 1.88 |
| %95 C.I. Difference | 0.88 (Lower), 1.96 (Upper) |
| $t_{49}$ | 31.799 |
| D*f* | 48 |
| Sig. (2-tailed) | .000 |
| Correlation | 0.970 |

**Table 6.** Paired sample t-test of total energy demand objective function Pareto-set

This study aimed to interpret the differences between two different optimizations' Pareto-sets, which were simulated with different weather conditions, e.g., current and future weather data. According to the optimizations, climate change has a dramatic impact on the selected educational building's energy consumptions and occupant comfort. Therefore the retrofitting processes should not be conducted by just considering the current weather conditions since this approach provides limited insight. The projected weather data contains higher outside dry bulb temperature and global irradiation values, which affects both energy demand and occupant comfort in buildings. The two optimizations' results showed that the optimization with $Y_{2\text{-Projected}}$ has lower values for the performance of convergence, but $Y_{1\text{-Projected}}$ was found higher in terms of higher dry-bulb temperature values. There were significant changes in both objective functions and the performance parameters of the optimizations. Therefore, the optimization or retrofit processes should consist of long periods of planning and should also include worst-case scenarios for better adaptation to future climate conditions.

## 5 CONCLUSION

In this paper, an approach for the comparative evaluation of the Pareto-sets conducted with current and future climate conditions for an educational facility is presented. For optimization, the main objectives were selected as total energy demand ($Y_2$) and discomfort hours ($Y_1$). The optimization results were found a high number of discomfort hours, according to Ashrae 55 [3], since the selected building was historic and had not any insulations on the envelope.

In the current weather data optimizations, $Y_{2\text{-Current}}$ had high values compared to $Y_{2\text{-Projected}}$, since the comparatively low outside dry-bulb temperatures caused high heating demands in the selected building. For the same reason, $Y_{1\text{-Current}}$ had lower values compared to $Y_{1\text{-Projected}}$. Oppositely, the optimization results for the projected weather data had higher $Y_{1\text{-Projected}}$ values and had lower $Y_{2\text{-Projected}}$ values due to the increased outside dry-bulb temperature and global irradiation (W/m$^2$). The Pareto-set of the two optimization processes were compared with the hypervolume indicator and statistical methods. By comparing the two Pareto-front results, the alteration occurring between the two optimizations was possible to be detected. In this way, the planned retrofit scenarios may be oriented to global climate change and may function more effectively for the educational facilities in the future.

**ACKNOWLEDGMENTS**
This research was partially supported by the Newton – Katip Celebi Fund, Grant No. 217M519, by the Scientific and Technological Research Council of Turkey (TUBITAK) and British Council, UK. Also, it was supported partially by the Middle East Technical University Scientific Research Grant BAP-02-01-2017-002. In this paper, the findings from Dino and Akgül's paper [8] were used thoroughly.

**REFERENCES**
1. Ainger, C., Bernier, P., and A. Fenner, R. Assessing the sustainability merits of retrofitting existing homes. *Proceedings of the ICE - Engineering Sustainability*, *163*, (2010), 197–207.
2. ASHRAE. ASHRAE climatic design conditions 2009/2013/2017. http://ashrae-meteo.info/index.php?lat=39.950&lng=32.883&place=%27%27&wmo=171300.
3. ASHRAE. *ASHRAE Standard 55-2004 -- Thermal Comfort*. 2004.
4. Auger, A., Bader, J., Brockhoff, D., and Zitzler, E. Hypervolume-based multiobjective optimization: Theoretical foundations and practical implications. *Theoretical Computer Science*, *425*, (2012), 75–103.
5. Belcher, S.E., Hacker, J., and Powell, D.S. Constructing design weather data for future climates. *Building Services Engineering Research and Technology*, *26*, (2005).
6. Berardi, U., Manca, M., Casaldaliga, P., and Pich-Aguilera, F. From high-energy demands to nZEB: The retrofit of a school in Catalonia, Spain. *Energy Procedia*, *140*, (2017), 141–150.
7. Deb, K., Pratap, A., Agarwal, S., and Meyarivan, T. A fast and elitist multiobjective genetic algorithm: NSGA-II. *IEEE Transactions on Evolutionary Computation*, *6*, 2 (April 2002), 182–197.
8. Dino, I.G. and Akgül, C.M. Impact of climate change on the existing residential building stock in Turkey: An analysis on energy use, greenhouse gas emissions and occupant comfort. *Renewable Energy*, *141*, (2019), 828–846.
9. Giouri, E.D., Tenpierik, M., and Turrin, M. Zero energy potential of a high-rise office building in a Mediterranean climate: Using multi-objective optimization to understand the impact of design decisions towards zero-energy high-rise buildings. *Energy and Buildings*, *209*, (2020), 109666.
10. Hashempour, N., Taherkhani, R., and Mahdikhani, M. Energy performance optimization of existing buildings: A literature review. *Sustainable Cities and Society*, *54*, (2020), 101967.
11. Hou, J., Liu, Y., Wu, Y., Zhou, N., and Feng, W. Comparative study of commercial building energy-efficiency retrofit policies in four pilot cities in China. *Energy Policy*, *88*, (2016), 204–215.
12. Jafari, A. and Valentin, V. An optimization framework for building energy retrofits decision-making. *Building and Environment*, *115*, (2017), 118–129.
13. Konstantinou, T. *Facade Refurbishment Toolbox*. 2014.
14. Sims, B.L. and Bakens, W.J.P. Next Page CIB Performance Based Building ( PeBBu ) Thematic Network. (2002), 1–8.
15. Sun, Y., Ma, R., Chen, J., and Xu, T. Heuristic optimization for grid-interactive net-zero energy building design through the glowworm swarm algorithm. *Energy and Buildings*, *208*, (2020), 109644.
16. Troup, L., Eckelman, M.J., and Fannon, D. Simulating future energy consumption in office buildings using an ensemble of morphed climate data. *Applied Energy*, *255*, (2019), 113821.
17. Witt, E., Lill, I., and Nuuter, T. Comparative Analysis of Current Guidance for the Evaluation of Building Retrofit Investments. *Procedia Economics and Finance*, *21*, (2015), 321–328.
18. Yigitcanlar, T. *Technology and the City: Systems, Applications and Implications*. Routledge, New York, 2016.
19. Zhai, Z.J. and Helman, J.M. Implications of climate changes to building energy and design. *Sustainable Cities and Society*, *44*, (2019), 511–519.
20. Zheng, Y. and Weng, Q. Modeling the effect of climate change on building energy demand in Los Angeles county by using a GIS-based high spatial- and temporal-resolution approach. *Energy*, *176*, (2019), 641–655.
21. DesignBuilder Software Ltd - Home. https://designbuilder.co.uk//.